

COMPUTATIONAL FLUID DYNAMICS SIMULATION OF INDOOR CLIMATE IN LOW ENERGY BUILDINGS Computational Set Up

by

Daniel RISBERG*, **Lars WESTERLUND**, and **J. Gunnar I. HELLSTROM**

Lulea University of Technology, Lulea, Sweden

Original scientific paper
<https://doi.org/10.2298/TSC1150604167R>

In this paper CFD was used for simulation of the indoor climate in a part of a low energy building. The focus of the work was on investigating the computational set up, such as grid size and boundary conditions in order to solve the indoor climate problems in an accurate way. Future work is to model a complete building, with reasonable calculation time and accuracy. A limited number of grid elements and knowledge of boundary settings are therefore essential. An accurate grid edge size of around 0.1 m was enough to predict the climate according to a grid independency study. Different turbulence models were compared with only small differences in the indoor air velocities and temperatures. The models show that radiation between building surfaces has a large impact on the temperature field inside the building, with the largest differences at the floor level. Simplifying the simulations by modelling the radiator as a surface in the outer wall of the room is appropriate for the calculations. The overall indoor climate is finally compared between three different cases for the outdoor air temperature. The results show a good indoor climate for a low energy building all around the year.

Key words: *CFD simulation, computational set up, indoor climate, low energy buildings, turbulence models, grid size, radiation, convection, radiator, near wall treatment*

Introduction

Investigation of the indoor climate in buildings can be performed with CFD technology. The air velocity and temperature can be predicted in all parts of the building with these simulations. Many studies have been made with the aim of predicting the indoor climate and heat losses in buildings using CFD software. Studies concerning computational set up for an entire low energy building are however missing in the literature. The first use of CFD to predict indoor airflow was made in 1974 [1]. In the last decades computer performance has increased rapidly and even extensive amounts of data are possible to handle with personal computers today. Together with improved software applications an increased use of CFD has occurred. The heat consumption for single-family houses (low energy buildings) decreases each year with more compact and better building envelope constructions. The concept low energy house refer to a building where the heat demand and peak load is significantly decreased compared to a building constructed according to Swedish National Board of Housing, Building and Planning's recommendations (BBP), different examples are Passive houses, Zero energy houses, and

*Corresponding author, e-mail: daniel.risberg@ltu.se

Mini energy houses [2]. A study evaluation of the 9 passive house in Sweden has shown that actual energy consumption on is 21-35 kWh/m² floor area [3] compared to around 80 kWh/m² for a conventional building.

Traditional methods of heating and ventilation may be overambitious in order to maintain a good indoor climate when the heat consumption is decreased. New efficient methods can maybe result in a similar indoor climate with less investment cost. Most of the published work with CFD simulations is focused on individual rooms with quite a high rate of supply air or using natural ventilation [4, 5]. A study regarding office ventilation schemes have simulated the indoor climate with an air change rate at 4 times [6]. In this study the flow rate is more realistic for single family houses at (0.35 l/s per m²) which are common standard in BBP. Simplifications such as to include the radiator in the outer wall and convective heat transfer coefficients through specified equations has been implemented, all in order to decrease the computational time. This has not been published earlier. Also simulations concerning a low energy building in subarctic climate is new.

Summarizing of different studies regarding turbulence models for both indoor and ventilation simulations have earlier been performed [7]. The conclusion of the paper is that many turbulence models have been used for indoor-air simulations and no universal model for turbulence can be chosen. The choice of turbulence model is mostly dependent on accuracy and time needed. Studies like [8] compare different $k-\varepsilon$ models where random number generation (RNG) show slightly better results as compared to the standard $k-\varepsilon$.

The heat losses through a building envelope are dependent on the conduction through the element, convection on both sides of the construction and radiation to/from the surfaces. The conduction part of a building element is easy to predict in a good way, but in order to predict an accurate model for indoor air-flow and temperatures the convective heat transfer is a difficult issue. The convective heat transfer coefficients for the isolated building surface are dominated by natural convection, and these values are hard to predict correctly both in CFD models and in experiments. There are many studies that have performed measurements of the heat transfer coefficient with large variations in the results. The study [9] concluded that the errors in his results in the best case are around 15%, [10] show that the mean values are around 1.4 W/m²K for a wall with no heating and around 1.6 W/m²K for a continuous heated wall. A review of empirical formulas for different isolated building surfaces has been published by [11].

The aim with this work was to establish computational set ups for simulations of the indoor climate in low energy buildings.

Methodology

In low energy buildings the convective forces are reduced since the heat transfer rates are so low when compared to ordinary buildings. This may affect the indoor climate in the building. Therefore, the volume of a one-family house is huge simplifications and a quite coarse mesh has to be introduced in order to make the simulation time more reasonable. A two room model was used in order to reduce the simulation time for the different tests to find the most suitable simulation set up. The elaborated set up was then finally used for an up scaled model of a whole house, this simulation was validated through measurements.

Simulation object

The simulated volume has two equal rooms with dimensions $W \times L \times H$: $2.0 \times 4.0 \times 2.5$ m connected through an opening (door), fig. 1. One room is ventilated with supply air, and the air-flow is then transferred to the other room where it leaves as exhaust air. The ventilation

ducts are placed close to the ceiling in the middle of each room. The heat supply through the radiators is simulated as a heat flux through the envelope face $W \times H: 1.0 \times 0.6$ m placed as one part of the short side of each room, a window $W \times H: 1.0 \times 1.0$ m is placed above the radiator and simulated in the same way as the radiator. The supply air-flow rate is equal to 0.35 l/s for every square metre of floor area, which is around 0.5 air change per hour (ACH). The value is according to BBP. In a room the occupied zone (volume people normally exploit) is defined as *The occupied zone is enclosed by two horizontal levels, one 0.1 m above floor level and the other 2.0 m above floor level, and a vertical level 0.6 m from the exterior wall or other external limit, or 1.0 m by windows and doors* [12]. The indoor climate according to BBP for operative temperature is at least 18 °C inside the occupied zone with a maximum difference of 5 °C inside this area and a highest temperature at 26 °C. Also the air velocities have a limit of 0.15 m/s for the winter season and for the relative humidity (RH) the critical value is 75% RH [12] in the occupied zone. A further demand is that the floor temperature in the building should not be lower than 16 °C. A vertical line from the floor to the ceiling was created in the room with exhaust air, fig. 1. The position was chosen to be in the occupied zone and where the influence from window and radiator was expected to be strongest. Results from simulations are presented along this line.

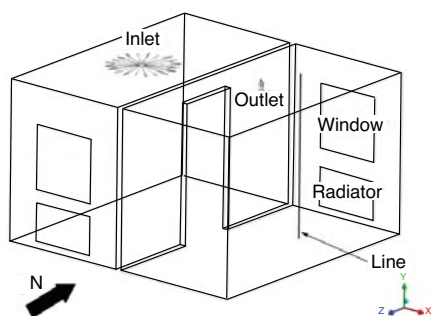


Figure 1. Simulated volume fin used in this study

+18 °C, a design temperature for a mixing supply device in the ventilation system. The room temperature was designed for a temperature of +20 °C. The transmission losses through the different building elements were calculated by multiplying the overall heat transfer coefficient with the air temperature difference. Other heat losses caused by infiltration through the envelope due to a pressure difference between the indoor and environmental conditions, it was set at a constant value of 0.1 ACH. Furthermore, heating of the supply air from inlet temperature to room temperature is made by the radiator. The summation of all heat losses in each room was calculated and applied as a positive heat flux from the radiator to obtain the design indoor temperature.

Numerical method

The numerical simulations were performed with the commercially available software ANSYS CFX 14.5. The programme solves partial differential equations numerically with a control volume based finite element method. The governing equations that are solved for are the conservation of mass, momentum, and energy. The discretisation method used for the simulations was a second order upwind scheme. For the turbulence numeric, first order upwind has been used in order to ease convergence. A convergence target of $1e-7$ for the scaled root mean square residuals was used for all the governing equations and turbulence model equations. For the summer case a value of $1e-4$ was used. The small value was chosen since the air temperature

The overall heat transfer coefficient, U , for the different building elements in a low energy building was manually calculated and representing of a typical low energy building in Sweden. The U -values are for outer walls 0.1 W/m²K, ceilings 0.085 W/m²K, ground 0.15 W/m²K, and windows 0.85 W/m²K. The simulations were made for three different cases of the outdoor air temperature for the Swedish town Lulea, according to Swedish Meteorological and Hydrological Institute, winter (-30 °C), summer (+20 °C), and for an annual mean outdoor temperature (+2 °C). This was done in order to examine the indoor climate during a year. The supply air temperature was set at

changed very slowly. The buoyancy effect was modulated according to the Boussinesq method, which uses a correlation where the density difference is calculated according to eq. (1), with a constant reference density ρ_{ref} and buoyancy reference temperature T_{ref} [13]:

$$\rho - \rho_{\text{ref}} = -\rho_{\text{ref}} \beta (T - T_{\text{ref}}) \quad (1)$$

The density of the air was also modelled as an ideal gas in order to investigate the influence from the chosen method.

Turbulence models and near wall treatment

For indoor conditions the air-flow is generally turbulent also for cases with low velocities [14]. Turbulent flow is difficult to solve directly, hence the use of a CFD software that utilizes a turbulence model to predict the fluctuations in the air motion. A common model is the k - ε model, which is a two equation model where one predicts the turbulent kinetic energy, k , and the other one predicts the eddy dissipation, ε . The standard k - ε method is a widely used turbulence model for these kinds of applications, which predicts the air-flow quite well in the simulation domain and is a good compromise between simulation results and computing time [13]. The RNG k - ε model is better adapted for flows with low Reynolds number because of an improved consideration of the effective viscosity at low Reynolds number [15]. The deviations between the two models are different constant values in the equations for described variables above and that in the turbulence equation standard the k - ε model uses a constant $C_{I\varepsilon}$ whilst the RNG k - ε model uses a function $C_{I\varepsilon\text{RNG}}$.

Two k - ω turbulence models, Standard and SST, were also introduced in the investigation of turbulence models. The k - ω models calculate the turbulent kinetic energy, k , together with the ω equation, which predicts the turbulent frequency. The SST model combines the k - ε and k - ω models utilizing the good behaviour of each model. The SST uses the ε formulation in the free stream and the ω formulation close to the wall. For the SST model a third wall scale equation is added.

The buoyancy was incorporated in the production term as a source term for the turbulent kinetic energy equation in all investigated turbulence models. Excluding buoyancy from the kinetic energy equation was also investigated in order to find the effects of its implementation. With the production term included a transient behavior appears, due to this a time dependent simulation had to be performed. This leads to long simulation times with only small differences in the results compared to neglecting the production term, mostly near the boundary regions. Therefore, in the simulation the standard setting was to exclude the buoyancy turbulence terms in order to get a stable solution.

The wall functions used to predict the near wall flow are the scalable wall functions. The improvement from the standard log law is that the singular separation points appear where the near flow velocity becomes zero, since the scalable wall function switches from a logarithmic approximation to a linear one for a y^+ value (dimensionless distance from the wall) of 11.06 [13]. In scalable definition the u_t is replaced by u^* , which describes a scalable velocity, in addition to scaling the y^+ value to a minimum value of 11.06. For the simulations with ω -based formulation the wall function chosen is the automatic wall function [13], since the ω -formulation requires a better resolution of the near wall region. In order to fully utilize the benefits of the SST-model a y^+ value close to 1 is recommended.

The convective heat transfer between wall and indoor air was treated by the software according to chosen wall functions. For the scalable wall treatment the convective heat flux was calculated:

$$q_w = \frac{rc_p u^*}{T^+} (T_w - T_f) \quad (2)$$

Boundary conditions

The boundary conditions are difficult to set properly in air-flow simulations. In this study the inlet of the supply device for the ventilation was modulated with a constant velocity of 2.23 m/s (which represent an air-flow of 0.35 l/s for every square metre of floor area) perpendicular to the inlet face, fig. 1. The outlet was set as a pressure outlet with constant pressure equal to the atmospheric pressure. Infiltration to the volume was neglected in the simulation due to the conservation of the mass in the software. The heat losses from this phenomenon were however included in the calculations and evenly distributed on envelope surfaces.

The envelope face was expressed with a no-slip condition and the thermal boundaries were described as a fixed heat flux on the faces based on *u*-values presented in section *Simulation object*. The values was set according to tab. 1, for the radiator the heat flux is represented for a simplified radiator surface. The radiation model is

Table 1. Heat flux for different outdoor temperatures

Building element	Heat flux (Winter case)	Heat flux (Annual mean case)	Heat flux (Summer case)
Wall	-5.45	-1.96	-0.45
Floor	-7.50	-2.70	-2.09
Ceiling	-1.53	-4.25	-0.34
Window	-15.3	-42.5	-3.05
Radiator	+408	+158	0.00

very important for the prediction of both the temperatures and the velocities in the flow domain [16]. Simulations with and without the radiation model were performed in order to investigate its influence. The P-1 radiation model [13] was used between the internal building surfaces. Inner walls were simulated as adiabatic and for all walls an emissivity of 0.9 was chosen. Window surfaces emissivity was set at 0.5, which represents a value of a low emissivity window on the market. For the radiators face an investigation with and without radiation was performed and an emissivity of 0.1 was used when radiation was activated. The low value used is due to the fact that the area of the radiator face was modulated smaller than its real size and the high surface temperature determined by the software. The radiant effect used was about 30% of total heat transfer rate according to Persson [17]. Investigation of simplifying the radiator as a face in the envelope surface or modelled as a real radiator located in the room was made with and without radiation involved.

For the summer case the solar radiation through the window was modulated as a heat flux that is representative of the solar load and placed at a direction in 45° towards the floor from the south window. The solar heat flux was calculated:

$$q_r = AG I_{sol} \sin(\phi) \quad (3)$$

According to this correlation the window directed to the south (positive z-direction in fig. 1) has a radiation heat flux of 100 W/m² with *G* of 0.5 and the window area is reduced to 0.8 m² because of area hidden from the frame.

Grid verification

For indoor climate simulations, as for all simulations the goal is to get a grid independent solution [14]. A small change in results during a grid refinement is almost impossible to avoid. Therefore, a grid dependency study was performed for the model, using the grid convergence index (GCI) together with an extrapolated curve according to Richardson extrapolation,

which was used to define the discretisation error [18]. The investigated grid sizes were chosen in order to get an almost constant value for the refinement ratio, r . Refinement of the mesh is done by minimizing the maximum size of the element in order to achieve a constant refinement rate. With use of an unstructured grid the ratio can be calculated according to eq. (4), following the approach by [19]. The parameter D describes the dimensions in the simulation, hence $D = 3$ in this case. The number of elements, N , depends on the grid size and the simulation geometry:

$$r = (N_{\text{fine}} / N_{\text{coarse}})^{\frac{1}{D}} \quad (4)$$

Investigated grid sizes with corresponding number of elements and a refinement ratio of $r = 1.41$ are: grid 1 = 883k elements, grid 2 = 314k elements, and grid 3 = 111k elements. Inflation layers (5 rows with a total depth of around 0.25 m) were used to resolve the convective air-flow close to the different surfaces. The zones close to the ventilation devices were meshed with a finer grid.

The most interesting variables for the indoor climate, velocity and temperature, respectively, were compared along the chosen line between floor and ceiling in the room with exhaust air, fig. 1. The difference γ in variable value ϕ was calculated according to eq. (5), ϕ_1 is the solution for the finer grid and ϕ_2 for the coarser grid. The same relationships were used for calculating γ_{32} :

$$\gamma_{21} = \phi_2 - \phi_1 \quad (5)$$

The order of GCI p was calculated:

$$p = \frac{1}{\ln(r_{21})} \left| \ln \left| \frac{\gamma_{32}}{\gamma_{21}} \right| + q(p) \right| \quad (6)$$

The parameter $q(p)$ in eq. (6) is equal to zero when the grid refinement ratio r_{21} equals r_{32} . When the value of γ_{32}/γ_{21} becomes less than zero, oscillating convergence appears, but if the value of γ_{32} or γ_{21} is nearly zero a sign of a mesh independency has been reached. An additional grid refinement was made when both γ_{21} and γ_{32} were nearly zero, which gave a total number of elements of 2.4 million elements. A global order of p was calculated as average value of all local values of p along the investigated line. This value of (p) was used in all further calculations. The approximated GCI value was calculated from eq. (7). The expression gives the error of the variable value for the finest grid in actual point:

$$GCI_{\text{fine}}^{21} = \pm \left(\frac{1.25e_a^{21}}{r_{21}^p - 1} \right) \quad (7)$$

The approximate relative error, e_a^{21} , was calculated according to:

$$e_a^{21} = \left| \frac{\phi_1 - \phi_2}{\phi_1} \right| \quad (8)$$

For the Richardson method an extrapolated solution ϕ_{ext}^{21} was calculated for an infinitely fine grid according to:

$$\phi_{\text{ext}}^{21} = \frac{r_{21}^p \phi_1 - \phi_2}{r_{21}^p - 1} \quad (9)$$

Measurements and validation

The chosen methods from the result section was validated for a single family building where measurements was performed during two months during March and April 2014. The sampling time was carried out on minute basis. The validated values carried out at an outdoor temperature of +6 °C. Five temperature sensors was placed according to the fig. 2 at a height of around 2 meters above the floor level. The sensors were of type pt1000 and according to manufacture measurement errors are in the ranges of ±0.4 °C. The heat supply through a water heating system was measured with a Kamstrup, Multical 402 device with an accuracy of 2%. The *U*-values of the building elements was the same as described for the two room model, at current outdoor temperature heat flux values according to tab. 2 was established.

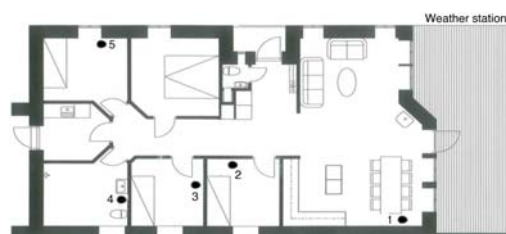


Figure 2. Sensor placement for indoor sensors, 1-5 – sensors

Results

The results were compared along the vertical line illustrated in fig. 1, since it gives a good representation of the occupied zone. The velocities have a value slightly higher than the mean velocity and the temperatures show a good representation of the average temperatures inside the house, with respect to different horizontal planes with varying heights.

Table 2. Heat flux for validated low energy building

Building element	Wall	Floor	Ceiling	Window/door
Heat flux [W/m ²] (+6 °C)	-1.92	-2.64	-1.5	-14.96

Grid refinement study

A grid independency study was performed for the case with mean outdoor temperature. Furthermore, the Boussinesq approximation, the standard *k-ε* turbulence model, scalable wall functions, a second order discretisation method and the radiation model included were used. Figure 3 show the velocity magnitude and fig. 4 the temperature for the different grid sizes chosen. The values close to the ceiling in fig. 3 depend on convective heat transfer. The velocity plot shows only small differences for the investigated grid sizes. The largest deviation arises for the simulation with the smallest amount of elements, fig. 3b. The local order of accuracy *p* for the velocity profile at different points is in the range 0.14-7.07 with an average of 2.55. The discretisation errors GCI from eq. (7), according to the velocity have a maximum value of about 20%. This high value is relative to a low velocity and corresponds to a maximum uncertainty in velocity of about ±0.015. The velocities are below the recommendation according to BBP in the occupied zone and should therefore not effectuate any discomfort in the indoor climate. The extrapolated curve fits to the case with 2400k grid cells.

For the temperature profile, fig. 4, the coarsest grid shows deviations compared to the other simulations. The remaining cases gave only small differences in temperature. The local order of accuracy is between 0.35 and 14.55 with an average of 7.11, see fig. 4b. The temperature values for the different grid sizes show oscillating convergence in 70% of the values. Since the difference in variable value *γ* for both *γ*₂₁ and *γ*₃₂ is nearly zero, an additional simulation was made with a refinement grid of 2400k cells. The variable temperature seems to show a grid independent solution for the case with around 314k elements and small discretisation errors. The extrapolated curve fits to the temperature curve for all cases except the coarsest case.

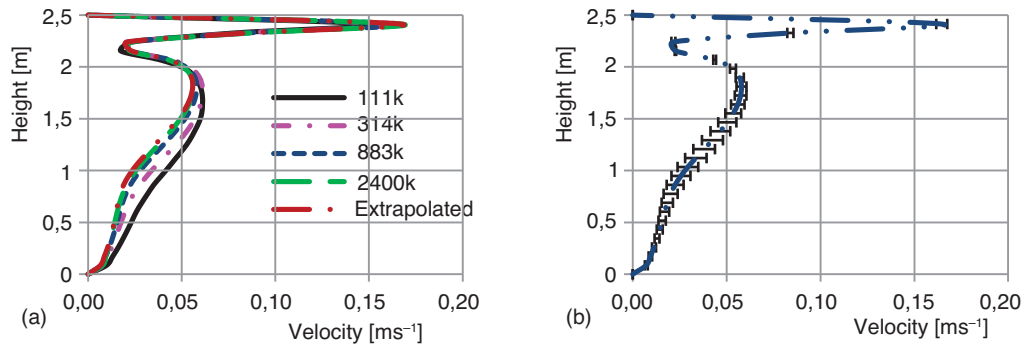


Figure 3. Velocity profile and discretisation error of velocities along studied line

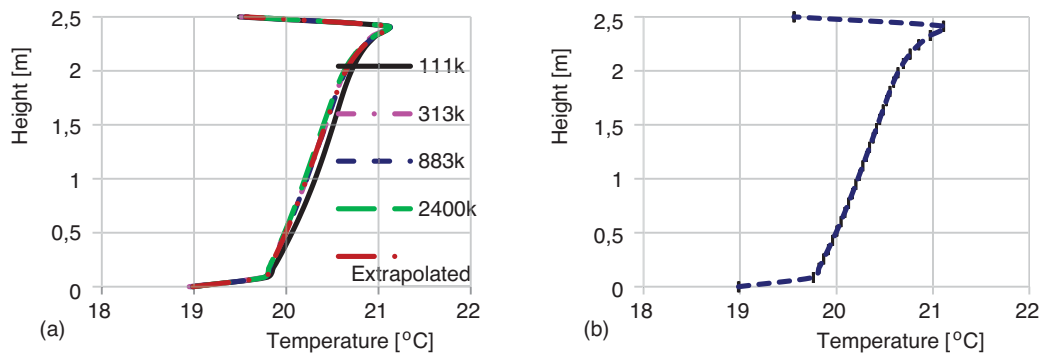


Figure 4. Temperature profile and discretisation error of temperature along studied line

According to the grid refinement study a grid with face length around 0.1 m and with 5 inflation layers (the case of 314k elements) gave acceptable results. For larger volumes like one-family houses, the central processing unit time with this grid size will also be tolerable. Hence, all further work in this paper was performed using this grid size. Investigation of two different buoyancy models, the Boussinesq approximation and ideal gas law behaviour was performed. All other settings that were used during the grid size study were applied. Along the actual line the difference was between 0-0.007 m/s for the velocity and 0-0.1 °C for the temperature. This small deviation between the two models and a faster convergence for the Boussinesq approximation motivated the choice of this buoyancy model for all the further work.

Turbulence models

Four different turbulence models were compared in order to investigate the most relevant model for CFD simulations of indoor climate. The turbulence models that were compared are widely used for indoor air-flow calculations. The same settings as used earlier were applied. Investigated turbulence models were two $k-\varepsilon$ models, Standard and RNG, and two $k-\omega$ models, Standard and SST. Velocities and temperatures are presented for the different turbulence models in fig. 5. The results show that the velocities deviate among the different models, while for the temperature the standard $k-\omega$ model creates the results that deviates the most.

The velocities in fig. 5 are lower than the recommendation by BBP, inside the occupied zone. The deviation among the models will therefore not affect the indoor climate, from a human perspective. The standard $k-\omega$ model shows the largest deviation and was therefore excluded.

All other models are possible to use for CFD simulation of the indoor climate in buildings, since they capture the main flow features for convective heat transfer from a radiator according to experiments [20, 21]. Even the hot negative buoyant jet that appears on the opposite wall from the radiator is detected, see fig. 9. The results from the standard $k-\varepsilon$ and $k-\omega$ SST show the smallest difference relative to each other. The average y^+ for the simulations is in the range of 9-11 with are far from the recommended values for the standard $k-\omega$ and the SST model. The computing time and convergence rate are fast for the standard $k-\varepsilon$ model and it is well used in all kinds of applications, hence this model was chosen for all further work.

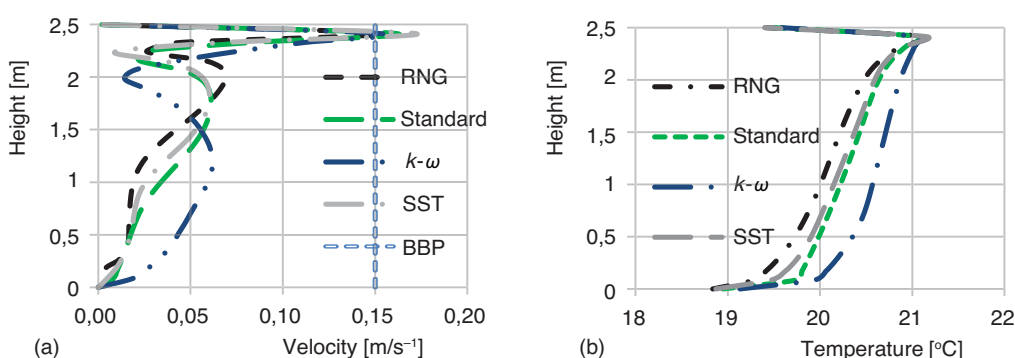


Figure 5. Velocity and temperature profile for the different turbulence models; (a) velocity, (b) temperature

Radiation effects

The effects of radiation in the simulation model are very important even though the temperature differences between the surfaces are small. Figure 6 shows the temperature profile along the investigated line for two cases with mean outdoor temperature boundaries, with and without radiation involved (radiator surface excluded). For the case without radiation the temperature drops to an unreasonably low value at the floor level. The velocities are very small and therefore more dense cold air is stacked up in this area. The indoor air temperature and velocity are almost the same at the other levels.

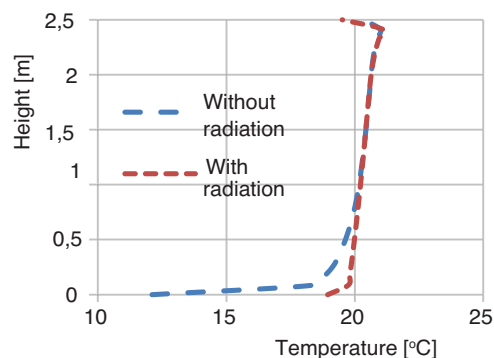


Figure 6. Surface and air temperature with and without radiation model included

Radiator modelling

Due to the irregular shape the radiator can not be meshed in its real shape since it would result in too many elements in the total volume of a house. A simplified radiator model, a face on the outer wall, was compared with a rectangular box ($W \times H \times D$: $1.0 \times 0.6 \times 0.05$ m) placed 0.05 m from the outer wall inside the room. Only convective heat transfer was assumed for these cases, and comparison where radiation was also included for both cases (30% of total heat flux) was performed. The air velocity and temperature along the line for the different cases are presented in fig. 7. A difference in velocity for the models appears, but the overall velocity is still small when compared with BBP. For the rectangular box with radiation the lowest velocities

appear due to the lower rate of convective heat flux from the radiator. A larger area compared to the face approach and radiation contribution is included. For the temperature the difference is small between the models but a smaller gradient appears for the rectangular box with radiation included. It can be concluded that modelling the radiator as a surface on the outer wall is sufficient when simulating the indoor climate in buildings.

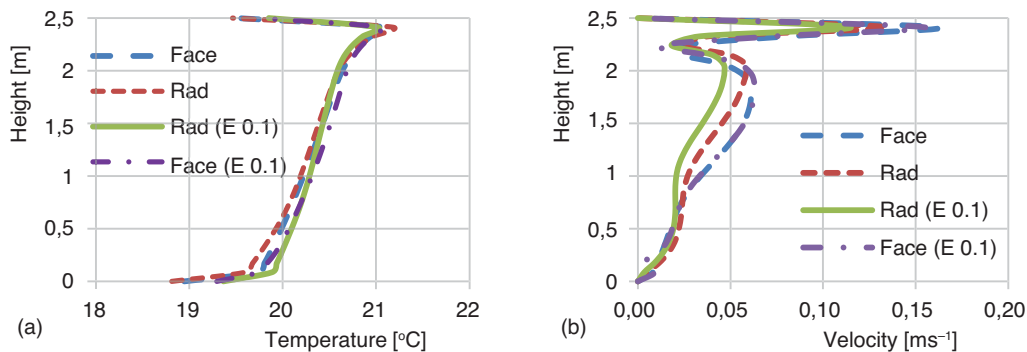


Figure 7. Air velocity and temperature along studied line for the different radiator models

Different environmental conditions

The indoor climate was simulated for three typical cases of the outdoor conditions representative of the north part of Sweden, with settings according to the previous study. A vertical plane in the middle of the room with supply air, going from the window to the opposite wall and from the floor to the ceiling, is presented in figs. 8-10. Planes located in the other room and at other positions indicate equivalent results.

The winter case with an outdoor temperature of $-30\text{ }^{\circ}\text{C}$, fig. 8, shows the highest air velocities above the radiator and along the ceiling towards the air supply unit. The highest air temperatures are also found in this area all due to buoyancy. The vertical temperature difference in the occupied zone of the plane is only $1.86\text{ }^{\circ}\text{C}$. This value is a good representation of the temperature gradient for the total volume of the two rooms. The air velocities in the plane show good mixing of the air and only low velocities. The heat supplied by the radiators was 245 W and with an area of 0.6 m^2 for each radiator.

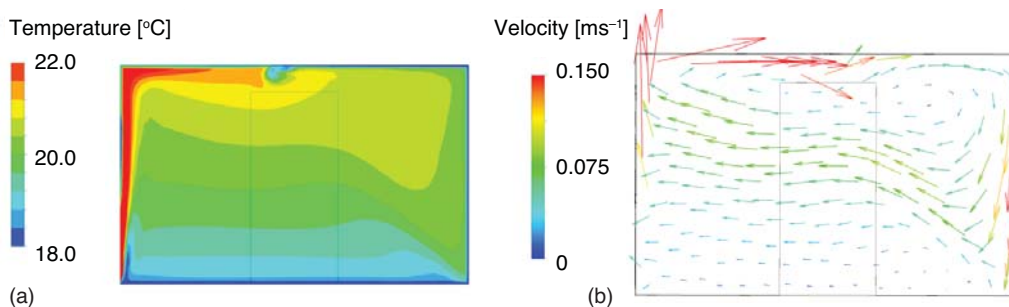


Figure 8. Conditions at a plane in the inlet room during the winter case; (a) velocity vector field and (b) temperature distribution

The indoor climate for the mean outdoor temperature case is presented in fig. 9. The radiators supply 95 W each for this case. The air movements show a similar pattern as for the winter case, but the magnitude of the velocity and air temperature difference is somewhat lower

than for the winter case because of the reduced heat exchange between the surfaces and the indoor air. The comparable temperature difference inside the occupied zone is 0.77 °C in the plane.

For the summer case the heating system is turned off, and the solar radiation is modelled as one part that describes the direct solar radiation. The direct solar radiation is calculated from eq. (3) and applied at the floor with a direction of 45° from the south window with an intensity of 100 W/m². The summer case is presented in fig. 10. The velocities inside the occupied zone are low and the air shows a good mixing. The temperature gradients in the plane show very small variations, 0.1 °C inside occupied zone of the plane, and the air temperature increases inside the simulation volume to a value of 24 °C in the occupied zone. The temperature is lower than 26 °C, which is the recommendation by the Swedish Government.

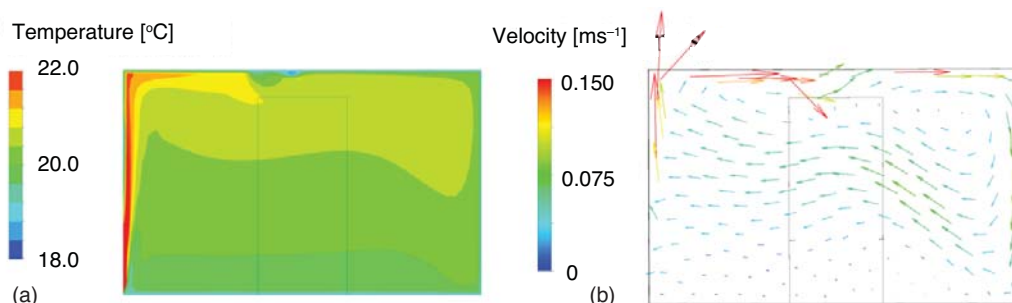


Figure 9. Conditions at a plane in the inlet room during the mean outdoor temperature case; (a) velocity vector field and (b) temperature distribution

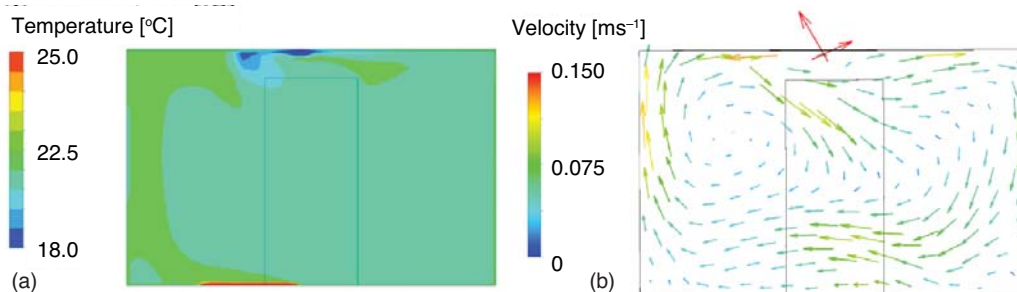


Figure 10. Conditions at a plane in the inlet room during the summer case; (a) velocity vector field and (b) temperature distribution

Average air temperatures in the room were calculated in horizontal planes every 0.5 m from the floor to the ceiling. In order to avoid the influence from the radiator instead of the level 0.5 m two levels 0.1 and 0.75 m above the floor were chosen. The mean surface temperature for the floor and the ceiling was also included in fig. 11. The temperature gradient inside the room is steeper for the winter case, which is what one would expect due to the increased heat transfer through the external surfaces. The deviation arises at the floor surface temperature and in the area up to 1.5 m above the floor.

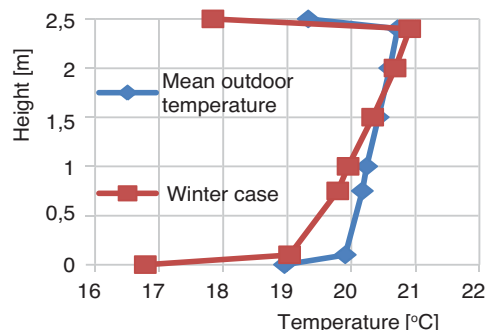


Figure 11. Average temperature gradient for two cases with different outdoor temperature during the heating season

For this low energy building the U -values are small and the temperature difference between floor and ceiling is low. The temperature gradient in the occupied zone is $1\text{ }^{\circ}\text{C}/\text{m}$ for the winter case and $0.4\text{ }^{\circ}\text{C}/\text{m}$ for the mean outdoor temperature case.

Validation

Measurements in a low energy building with one family resident have been performed. The building was located in the northern part of Sweden. To minimize the influence of the inhabitants the validation was done at early morning at 5 a. m. The air temperature in one point in each of the five rooms was measured. The outdoor temperature was $+6\text{ }^{\circ}\text{C}$. Figure 12 shows measured and simulated values according to chosen CFD model of the air temperature in each room. Room 1 is the open planned living room and kitchen, rooms 2, 3, and 5 are bedrooms, and room 4 is the toilet. The difference is at maximum $0.75\text{ }^{\circ}\text{C}$, the simulated values are not including internal heat from the people sleeping in rooms 2, 3, and 5.

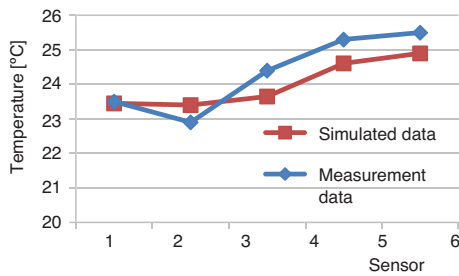


Figure 12. Validation of CFD simulation (for sensors number see fig. 2)

Discussion

In CFD simulations very specific problems are often studied, with large gradients in temperature and velocities and small grid cells are therefore normally used. When an entire building is to be simulated, an acceptable result can be established also for a coarse grid solution, since the gradients are small. A coarse grid is also necessary because of the large volumes investigated.

The scalable wall functions calculation of the surface temperature for the radiator seems to be high, but the air temperature in the first node point is feasible. A high surface temperature also causes an emissivity value that is fairly low in order to not overestimate the heat transfer mechanism.

A radiation model is very important to include in the simulation. The effect shows mainly on the floor temperature. Without radiation the floor temperature decreases to unreasonably low values due to buoyancy and low convective heat transfer rate. To increase the indoor climate the temperature on the floor and up to a level of 1.5 m above the floor should be raised.

With higher temperatures in this area the indoor climate can probably be preserved even if the air temperature inside the room decreases, *i. e.* the heat losses can be decreased even more.

Conclusions

The CFD simulation can be used to predict the indoor climate in buildings. For simulations of the indoor climate it is important to capture the main flow velocities and temperatures in the building.

A grid independency study shows that an acceptable number of elements is around 300k elements for the chosen simulation volume. This value represents a grid edge size of around 0.1 m to get an accurate result according to the discretisation errors.

The buoyancy effect must be included in the simulations of the indoor climate, and the Boussinesq approximation fulfils that demand. A comparison of different turbulence models shows quite small deviations, although the standard $k-\omega$ model shows the largest deviation. The standard $k-\varepsilon$ model should be used since it is numerical stable and gives good results with reasonable central processing unit time.

The velocities are much lower in the occupied zone as compared to the maximum acceptable value according to BBP, therefore the deviation between the models will not affect the indoor climate from a human perspective.

Radiation between building surfaces have a substantial impact on the temperature level for indoor climate simulations. Simulations with radiation excluded show too low temperatures on the floor. For a simulation with the mean outdoor air temperature a floor temperature around 12 °C was obtained, while with radiation included a floor temperature of around 19 °C was achieved. Radiation from the heat source has a small effect on the temperature gradient inside the occupied zone. However, the gradient in the room becomes straighter with radiation included in comparison with only involving convective heat transfer for the radiator. Simplifying the simulations by modelling the radiator as a surface in the envelope of the room is appropriate for simulations of the overall indoor climate.

Simulations of the climate inside the room with environmental winter conditions of -30 °C show low air velocities and temperature differences of less than 2 °C. When the outdoor temperature increases to +2 °C the indoor air temperature difference is only 0.8 °C. The temperature gradient inside the occupied zone decreases with increasing outdoor air temperature, which would be expected. The small difference originates from small heat fluxes through the envelope (low energy building). For the summer case (outdoor air temperature +20 °C) with direct solar radiation no temperature gradient appears inside the occupied zone due to the direct solar radiation and is detected by the floor. The average indoor air temperature was +20 °C except for the summer case where it rose to +24 °C. Future work in which the results of this work are incorporated, is to be implemented for a total building and validated in detail. To connect to the residents also comfort parameters will be studied in order to show the powerful tool that CFD constitutes.

Acknowledgment

This work has been carried out thanks to funding from the County Administrative Board of Norrbotten.

Nomenclature

A – surface area, [m²]
 ACH – air change per hour, [h⁻¹]
 c_p – specific heat capacity, [Jkg⁻¹°C⁻¹]
 D – dimensions in the simulation volume, [m]
 e_a^{21} – relative error
 G – transmission of solar radiation through the window
 GCI – grid convergence index
 I_{sol} – solar radiation intensity, [Wm⁻²]
 k – kinetic turbulent energy, [m²s⁻²]
 p – order of GCI
 q_r – radiation flux through the window, [Wm⁻²]
 q_w – heat flux, [Wm⁻²]
 r – grid refinement ratio

T_f – near wall fluid temperature, [°C]
 T_{ref} – reference temperature, [°C]
 T_w – wall temperature, [°C]
 U – overall heat transfer coefficient, [Wm⁻²K⁻¹]

Greek symbols

β – coefficient of expansion, [°C⁻¹]
 γ – difference between variable values
 ε – turbulent eddy dissipation, [m²s⁻³]
 ρ – density, [kgm⁻³]
 ρ_{ref} – reference density, [kgm⁻³]
 ϕ – variable value
 φ_{ext}^{21} – extrapolated solution
 ω – turbulent frequency, [s⁻¹]

References

- [1] Nielsen, P. V., Flow in Air-Conditioned Rooms. Ph. D. thesis, Technical University of Denmark, Copenhagen, 1974

- [2] ***, SCNH. FEBY12 Report, Specification of Requirements for Zero-Energy Houses, Passive Houses and Minienergyhaus, (in Swedish), 2012
- [3] Rohdin, *et al.*, Experiences from Nine Passive Houses in Sweden – Indoor Thermal Environment and Energy Use, *Building and Environment*, 71 (2014), Jan., pp. 176-185
- [4] Lin, Z., *et al.*, Validation of CFD Model for Research into Displacement Ventilation, *Architectural Science Review*, 48 (2005), 4, pp. 305-316
- [5] Allocca, C., *et al.*, Design Analysis of Single-Sided Natural Ventilation, *Energy and Buildings*, 35 (2003), 8, pp. 785-795
- [6] Zhuang, R., *et al.*, CFD Study of the Effects of Furniture Layout on Indoor Air Quality under Typical Office Ventilation Schemes, *BUILD SIMUL*, 7 (2014), 3, pp. 263-275
- [7] Zhai, Z. J., *et al.*, Evaluation of Various Turbulence Models in Predicting Airflow and Turbulence in Enclosed Environments by CFD: Part 1–Summary of Prevalent Turbulence Models, *Hvac&R Research*, 13 (6), (2007), 6, pp. 853-870
- [8] Rohdin, P., Moshfegh, B., Numerical Predictions of Indoor Climate in Large Industrial Premises – A Comparison between Different $k-\epsilon$ Models Supported by Field Measurements, *Building and Environment*, 42 (2007), 11, pp. 3872-3888
- [9] Wallenten, P., Convective Heat Transfer Coefficients in a Full-Scale Room with and without Furniture, *Building and Environment*, 36 (2001), 6, pp. 743-751
- [10] Delaforce, S. R., *et al.*, Convective Heat Transfer at Internal Surfaces, *Building and Environment*, 28 (1993), 2, pp. 211-220
- [11] Khalifa, A. J., N., Natural Convective Heat Transfer Coefficient – a Review: II. Surfaces in Two- and Three-Dimensional Enclosures, *Energy Conversion and Management*, 42 (2001), 4, pp. 505-517
- [12] ***, Boverket, BFS 2011:26, BBR 19, Boverket, 2011
- [13] ***, Ansys. ANSYS CFX-14.5 Solver Theory Guide. Ansys, inc. 2012
- [14] Chen, Q., Xu, W., A Zero-Equation Turbulence Model for Indoor Airflow Simulation. *Energy and Buildings*, 28 (1998) 2, pp. 137-144
- [15] Stamou, A., Katsiris, I., Verification of a CFD Model for Indoor Airflow and Heat Transfer, *Building and Environment*, 41 (2006), 9, pp. 1171-1181
- [16] Sorensen, D. N., Nielsen, P. V., Quality Control of Computational Fluid Dynamics in Indoor Environments, *Indoor Air*, 13 (2003), 1, pp. 2-17
- [17] Persson, T., Energy Savings with Pellet Stoves and Solar Heating in Direct Heating Single-Family Homes, (in Swedish), Licentiate Dissertation, Dalarna University, School Technology and Business Studies, Environmental Engineering, KTH, Energiteknik, Stockholm, 2004
- [18] Celik, I. B., *et al.*, Procedure for Estimation and Reporting of Uncertainty Due to Discretization in CFD Applications, *ASME J. Fluids Engin*, 130 (2008), 7, pp. 078001-078004
- [19] Roache, P. J., Perspective: A Method for Uniform Reporting of Grid Refinement Studies, *ASME J. Fluids Engin*, 116 (1994), 3, pp. 405-413
- [20] Howarth, A. T., The Prediction of Air Temperature Variations in Naturally Ventilated Rooms with Convective Heating, *BSE&T*, 6 (1985), 4, pp. 169-175
- [21] Riederer, P., Thermal Room Modelling Adapted to the Test of HVAC Control Systems. Ph. D. thesis, Ecole des Mines de Paris, Paris, 2002